On the Ideal Gas Law for Crowds with High Pressure

Zexu Li and Lei Fang*
Department of Civil and Environmental Engineering,
University of Pittsburgh, Pittsburgh, Pennsylvania 15261, USA
(Dated: March 9, 2024)

Active particle systems, such as human crowds, are out of equilibrium posing a significant challenge in identifying a suitable equation of state. However, several previous observations suggest that a crowd's speed distribution may conform to a two-dimensional Maxwell-Boltzmann distribution under certain yet-to-be-determined conditions. Our research uncovers that the divergence between the fluctuation velocity magnitude's probability density function and its best 2D Maxwell-Boltzmann fit diminishes in a power-law fashion with decreasing collision time scale between individuals. These findings are robustly supported by both experimental data and simulations with diverse boundary conditions and force potentials. The equilibrium characteristics of crowds are interpreted through a canonical ensemble framework. Furthermore, we show that high pressure indicates equilibrium characteristics in human crowds. Remarkably, we reveal the ideal gas law for human crowds without resorting to any behavior assumption. We demonstrate the predictive capability of the ideal gas law on both observational and modeling data. Our research highlights a new pathway to explore and validate traditional thermodynamic quantities and laws in the setting of high-pressure human crowds, advancing our understanding of active matter systems.

I. INTRODUCTION

Collective humans exhibit a range of behaviors. For instance, individuals naturally form lanes in pedestrian traffic, demonstrating an instinctual organization [1]. Alternatively, panic situations, such as emergency evacuations, can lead to uncontrolled jamming at exit points due to heightened stress [2]. Under specific social settings, Mexican waves were observed at sporting events. There are two major perspectives in approaching human crowds—microscopic (individual level) perspective and the macroscopic (group level) perspective. From a microscopic perspective, researchers believe that individuals follow a set of rules either consciously or subconsciously, and the microscopic interactions percolate through scales to generate larger-scale collective crowd behaviors, such as lane formation [3, 4] and heading alignments [5]. On the other hand, researchers taking a macroscopic perspective focused on group-level properties. They believed that extracting individual interaction rules from observations of group behavior was a complex and nonlinear inverse problem [6], and sometimes the inverse problem could even be ill-posed because the same macroscopic behavior could generate from different rule sets [7]. Despite the two distinctive perspectives, the two perspectives are complementary, especially for the human crowd [8, 9]. It is shown that microscopic interactions of humans can be surprisingly well reproduced computationally, and the resulting macroscopic collective behavior is not only qualitatively correct but also quantitatively similar. The concept of "active matter" fittingly characterizes human crowds, in which individuals, as constituent elements, convert internal energy into motion, thus operating out of equilibrium [6, 10–16]. Active matter systems, unlike passive ones, continually consume energy to drive their own dynamics, thereby making the utilization of conventional thermodynamic methods formidable.

Nonetheless, few prior studies have postulated that such crowds can display equilibrium characteristics under specific yet unidentified conditions [17, 18]. For instance, evidence of this phenomenon is exemplified in mosh pits, where the observed speed distribution aligns remarkably well with the two-dimensional (2D) Maxwell-Boltzmann distribution [18].

The endeavor to identify under which conditions human crowds display equilibrium characteristics, and subsequently, the nature of these characteristics, is valuable as it can elucidate a clear pathway toward uncovering the analogous thermodynamic theory governing such crowds. This finding could pave the way for in-depth investigation and verification of traditional thermodynamic concepts within the domain of the human crowd. We motivate our paper with three critical questions. Firstly, why do human crowds, an inherently non-equilibrium system, exhibit characteristics consistent with thermodynamic equilibrium? Secondly, what state variable can reliably indicate the manifestation of equilibrium behavior within a crowd? Lastly, can we formulate an equation of state for such crowds?

In this paper, we reveal that human crowds tend towards exhibiting equilibrium characteristics, where the individuals' fluctuation velocity magnitude distribution conforms to a 2D Maxwell-Boltzmann distribution, as the collision timescale between each other decreases. This result is not motion case dependent and holds for different assumed social forces between individuals. Surprisingly, these equilibrium properties can persist even in the presence of strong self-propulsion for individuals. In addition, we show that there is a power law relationship between collision time scale and pressure, suggesting that higher pressure indicates equilibrium behavior

* lei.fang@pitt.edu

within human crowds. Under high pressure, we reveal that the translational degrees of freedom (d.o.f.) follows the equipartition theorem. The equilibrium characteristics of the human crowd system directly imply the ideal gas law for crowds. To demonstrate the predictive ability of the ideal gas law, we collected 10^2 hours of video of dense crowd observational data on YouTube.com that were filmed from a suitably high position [19]. We find that we can predict the pressure very well in all the video data. In addition, we drive a crowd in a thermodynamic cycle in a crowd model and demonstrate the predictability of the ideal gas law for human crowds under high pressure.

Our results are organized as follows. In Sec. II, we present the data used for our study, detailing our experimental data and the models we employed. We show that the crowd exhibits equilibrium characteristics as the collision time scale decrease for all experimental and modeling data. In Sec. III, we explain why human crowds can sometimes exhibit equilibrium characteristics and reveal that human crowds exhibit equilibrium characteristics when pressure is high. Moreover, we reveal that human crowds under high pressure follow the equipartition theorem. We establish and verify the ideal gas law of crowds with high pressure in Sec. IV. Lastly, we conclude our paper in Sec. V.

II. EXPERIMENTAL AND MODELING DATA

We first describe the experimental and modeling data for this paper. We use both experiments and agent-based modeling to show that the individuals' fluctuation velocity magnitude distribution becomes more similar to the 2D Maxwell-Boltzmann distribution ($f(\|\mathbf{v}'\|) = \frac{2\|\mathbf{v}'\|}{k_B T} e^{-\frac{\|\mathbf{v}'\|^2}{k_B T}}$) as the collision time scale ($t_c = 1/(2\rho r\langle\|\mathbf{v}'\|\rangle)$) between individuals decreases, where $\langle\rangle$ indicates ensemble mean, and $\|\|$ is the L2 norm, ρ is crowd density, r is the mean distance between individuals and $\mathbf{v}'$ is the fluctuation velocity. We used bottleneck and unidirectional cases with large population densities.

A. Experimental Data

For experiments, we utilize the data from evacuation experiments carried out by Feliciani *et al.* [21] and unidirectional flow executed by Cao *et al.* [22]. Seven cases in bottleneck evacuation experiments and nine cases in unidirectional flow experiments were analyzed. The data sets consist of videos and corresponding individual's trajectories. Based on trajectories, velocity time series can be derived via a Gaussian derivative kernel. Gaussian derivative kernels were widely used in experimental research of Lagrangian turbulence to filter out high-frequency noise while taking derivative [23–25]. After applying Gaussian derivative kernels, smoothed velocity along the trajectories is obtained (Supplementary materials).

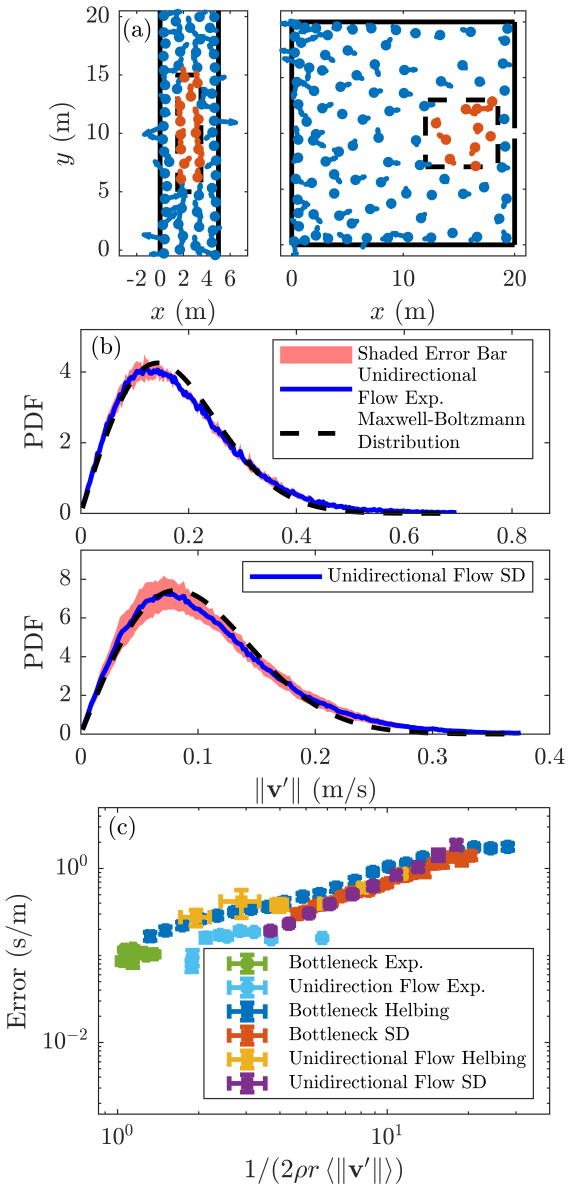

FIG. 1. (a) The bottleneck and unidirectional flow cases simulated by social distance model [20]. The arrow is the instantaneous velocity. The dashed square is the interrogation area. Our result holds well for a range of interrogation areas. (b) PDFs for fluctuation velocity magnitude (blue line) and the corresponding best fit to a 2D Maxwell-Boltzmann distribution (black dashed lines). The shaded area represents the error bar with a 95% confidence interval. (c) Collision time scale (t_c) versus the mean squared error between fluctuation velocity magnitude PDFs and their best 2D Maxwell-Boltzmann fit. A power law relationship between the t_c and error indicates that the system behaves more like an equilibrium system when t_c decreases.

B. Modeling Data

In high-density crowds, the physical interactions between each body and the simultaneous collective desire of reaching a point of interest dominate crowd dynamics and social attributes of pedestrians is minimized. Thus, we used the Helbing-Molnar model [26] and a social distance (SD) model [20] for crowd modeling. These models have been explained in detail elsewhere [10, 20, 26, 27], and we only introduce this model briefly. The models assume that there are N individuals i in the crowd with locations $\mathbf{r}_i(t)$ and velocities $\mathbf{v}_i(t)$. Each individual also has a desired speed v_i^D and is limited by a maximum speed v_i^{max}. The change in an individual's speed is interpreted as the consequence of the summation of three major "social forces" on the individual. The individual's acceleration is given by

$$\frac{d\mathbf{v}_i(t)}{dt} = \frac{v_i^D \mathbf{e}_i(t) - \mathbf{v}_i(t)}{\tau} + \sum_{j \neq i} \mathbf{F}_{ij} + \mathbf{F}_{iW}, \qquad (1)$$

where individuals intend to move in the direction of unit vector $\mathbf{e}_i(t)$ with velocity magnitude v_i^D in absence of interactions, and τ is the relaxation time. The $\mathbf{e}_i(t)$ is defined as $\mathbf{e}_i(t) = \frac{\mathbf{r}_i^D - \mathbf{r}_i(t)}{\|\mathbf{r}_i^D - \mathbf{r}_i(t)\|}$, where $\mathbf{r}_i^D$ is the location of the desired destination. $\mathbf{F}_{ij}$ represents the repulsive interaction between individual i and j, and $\mathbf{F}_{iW}$ describes the interaction between individual i and the wall. For interaction between individuals and walls, we have chosen the function

$$\mathbf{F}_{iW}(\mathbf{r}_{iW}) = -\nabla_{\mathbf{r}_{iW}} U_{iW}(\|\mathbf{r}_{iW}\|), \qquad (2)$$

where U_{iW} is a repulsive monotonic decreasing potential, and $\mathbf{r}_{iW} = \mathbf{r}_i - \mathbf{r}_W$ with $\mathbf{r}_W$ defined as the closest point on the wall to the individual. For the repulsive potential U_{iW}, we follow the Helbing and Molnar's form [26]: $U_{iW}(\|\mathbf{r}_{iW}\|) = U_{iW}^0 e^{-\|\mathbf{r}_{iW}\|/R}$, where U_{iW}^0 and R are constants.

For the interactions between the particles, we use

$$\mathbf{F}_{ij}(\mathbf{r}_{ij}) = -\nabla_{\mathbf{r}_{ij}} V_{ij}(\|\mathbf{r}_{ij}\|). \qquad (3)$$

The Helbing-Molnar model and social distance model use different potentials between individuals. The Helbing-Molnar model uses exponential potential $V_{ij}(\|\mathbf{r}_{ij}\|) = V_{ij}^0 e^{-\|\mathbf{r}_{ij}\|/R_{i,j}}$, where V_{ij}^0 and $R_{i,j}$ are constants, and $\mathbf{r}_{ij} = \mathbf{r}_i - \mathbf{r}_j$. Social distance model uses Lennard-Jones-like potential [20]

$$V_{ij}(\|\mathbf{r}_{ij}\|) = \epsilon\left(\left(\frac{\sigma}{\|\mathbf{r}_{ij}\|}\right)^{2n} - \left(\frac{\sigma}{\|\mathbf{r}_{ij}\|}\right)^{n}\right), \qquad (4)$$

where ϵ, σ and n are scalar constants. When the distance between two particles is equal to σ, the inter-particle potential is zero, and σ is interpreted as the "soft diameter" of the particle. Moreover, n represents the "hardness" of spheres; that is, as n increases, the repulsive force will increase more sharply when two individuals get closer. In the context of the crowd model, n represents individuals' priority to keep social distance ~~(SD)~~ over other factors, such as the desire to reach a destination. As n decreases, individuals tend to have a lower priority of keeping social distance, and violations of the prescribed social distance increase. The repulsive force is scaled by a linear factor ϵ [20].

We simulated both bottleneck and unidirectional flow cases with both force potentials. In each case, we simulated with $v_i^D = 0.7$ m/s and $v_i^{max} = 1.3 \times v_i^D = 0.91$ m/s. The pre-factor 1.3 is inherited from previous crowd literature [26]. For the bottleneck case, we simulate a crowd of 100 individuals exiting a room of 20 m by 20 m via a door of 0.92 m width. For the unidirectional flow case, we simulate a crowd of 100 individuals walking through a 20 m long corridor with a 5 m width.

We used the same parameters for the wall potential where $U_{iW}^0 = 10\ \mathrm{m}^2/\mathrm{s}^2$ and $R = 0.2$ m. As for the Helbing and Molnar's potential, the parameters are set as, $V_{i,j}^0 = 2.1\ \mathrm{m}^2/\mathrm{s}^2$, $R_{i,j} \in [0.2\ \mathrm{m}, 2.5\ \mathrm{m}]$, and $\tau \in [0.5\ \mathrm{s}, 6.5\ \mathrm{s}]$. Furthermore, we use the following parameters in the social distance model, $\epsilon = 3$, $n = 0.5$, $\sigma \in [0.2\ \mathrm{m}, 2.3\ \mathrm{m}]$ and $\tau \in [2.3\ \mathrm{s}, 7.25\ \mathrm{s}]$. The time step utilized in these two models is 0.02 s.

III. EQUILIBRIUM CHARACTERISTICS

The instantaneous velocity tells us little about the interaction between individuals. Instead, we focus on the individual's fluctuation velocity. Let us introduce for each individual i the fluctuation velocity around the mean is defined as [28, 29]

$$\mathbf{v'}_i(t) = \mathbf{v}_i(t) - \frac{1}{N}\sum_{k=1}^{N} \mathbf{v}_k(t), \qquad (5)$$

where $\mathbf{v}_k(t)$ is the instantaneous velocity, and N is the number of individuals at time t in the region of interest.

Two snapshots of the instantaneous velocity field within the interrogation area are shown in Fig. 1 a. In the selected region, we collect all the individual fluctuating velocities over time, resulting in a probability density function (PDF) curve for a single case. In Fig. 1 b, we plot the PDF of fluctuation velocity magnitude averaged over separated PDF curves from 9 experimental and hundreds of numerical cases (with SD potential) for unidirectional flow. For each PDF curve, we fit a series of 2D Maxwell-Boltzmann distributions. The error is defined as the mean squared error between the observed PDF curve and the best fit. In Fig. 1 c, we show that the mean squared error decreases as the collision time scale decreases for both experimental and modeling crowds. For the experimental dataset of unidirectional pedestrian flow, we have nine sets of data, so there are nine points in the graph, while error bars characterize the deviation over time. For simulation data, we have hundreds of cases. For the sake of presentation, we split

the range of collision timescale into several segments and computed the mean error and mean collision timescale for each segment. We find that this result is independent of the force potential we use in the model and it is also independent of the motion cases.

A. Equilibrium Characteristics via Canonical Ensemble

Why does the human crowd, an inherently non-equilibrium system, exhibit equilibrium characteristics? We find that the equilibrium characteristic is solely due to a large collision frequency, i.e., a small t_c, which is the mean free path $1/(2r\rho)$ divided by the mean fluctuation velocity magnitude $\langle\|\mathbf{v}'\|\rangle$. This can be understood via canonical ensemble [30]. In a crowd system, along one direction, a focal individual is a system while the rest of the crowd is the reservoir. With a small collision time scale, the temperature ($T \propto \langle\mathbf{v}'^2\rangle$) of the system is constant over a sufficient amount of collisions. In addition, collisions between individuals are near elastic collisions, and the constant collision exchanges energy between the system and the reservoir, making the probability of the system kinetic energy along one direction to be $P(E_k) \propto e^{-E_k/k_BT}$ (see supplementary material). Using the kinetic theory of gases, we will find that the fluctuation velocity magnitude follows the 2D Maxwell-Boltzmann distribution. As the energy exchange between the system and reservoir is more frequent, the crowd will behave more similarly to the equilibrium counterpart (Fig. 1 c).

The collision time scale should be much smaller than the time scale of the system's temperature so that a sufficient amount of collision can happen before the system temperature change, and, thus, one of the assumptions in the canonical ensemble is fulfilled. On the other hand, if a crowd system has a temperature that varies too quickly compared with the collision time scale, the picture of the canonical ensemble is no longer suitable. Thus, the crowd system lost its equilibrium characteristics. In our case, when crowd density is high, the variation of the temperature is pretty slow, and we will not include the temperature variation in our discussion.

The fact that the equilibrium characteristic is solely due to small t_c is somewhat surprising. Away from the wall, conceptually, there are two time scales: τ and t_c. The τ is the time scale for individuals to adjust their velocity toward the desired direction and magnitude that is shown in the first term on the right-hand side of Eqn. 1. This is the self-propelling part of the active particle system. In other words, individuals are not passively colliding with each other but instead, drive themselves toward their point of interest. The energy for the self-proportion comes from other sources, adding kinetic energy to the system. The self-propelling part drives the system out of equilibrium. On the other hand, t_c is the time scale of the passive part of the active particle system. Intuitively, one may believe that the equilibrium characteristics will

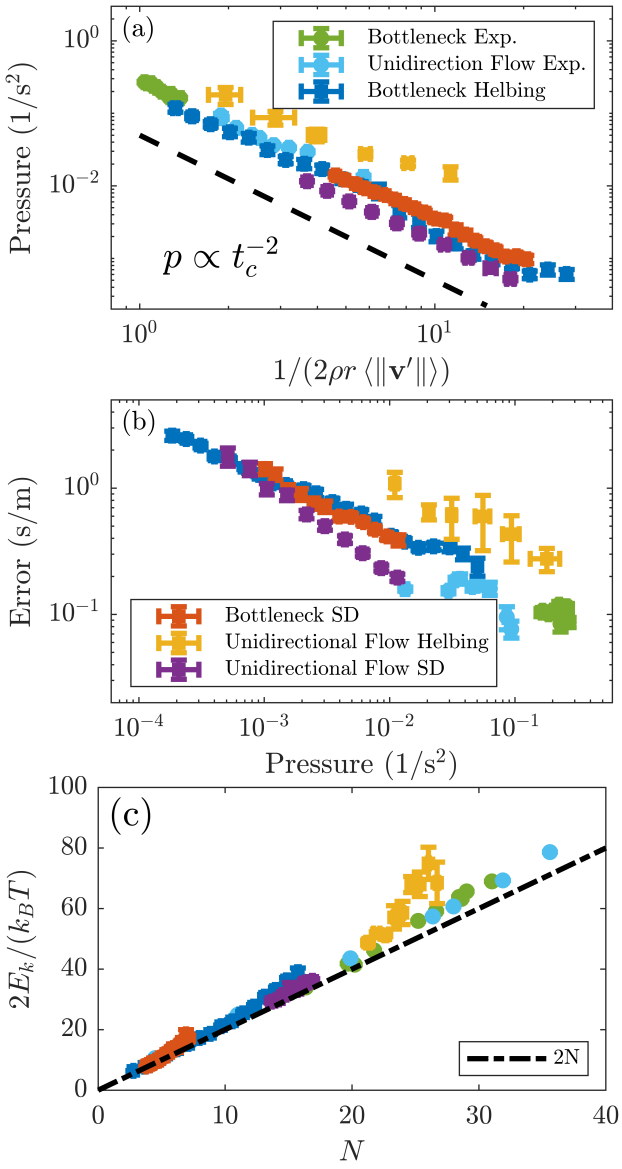

FIG. 2. (a) The power-law relationship between pressure and t_c. The predicted $p \propto t_c^{-2}$ is shown in the black dashed line. (b) The pressure of the crowd versus mean squared error between fluctuation velocity magnitude PDFs and their best 2D Maxwell-Boltzmann fit. A power law relationship exists between the pressure and the mean squared error of the fluctuation velocity magnitude PDFs and their optimal 2D Maxwell-Boltzmann fit. This indicates that the system increasingly behaves like an equilibrium system as pressure rises. (c) The total kinetic energy normalized by $1/2k_BT$ as a function of the number of individuals varied by varying interrogation domain sizes and locations. For crowds with high pressure, the total normalized kinetic energy is well approximated by the $2N$ (black dashed line), indicating that there are two translational d.o.f. in the system. Error bars with 95% confidence interval are shown in the figure.

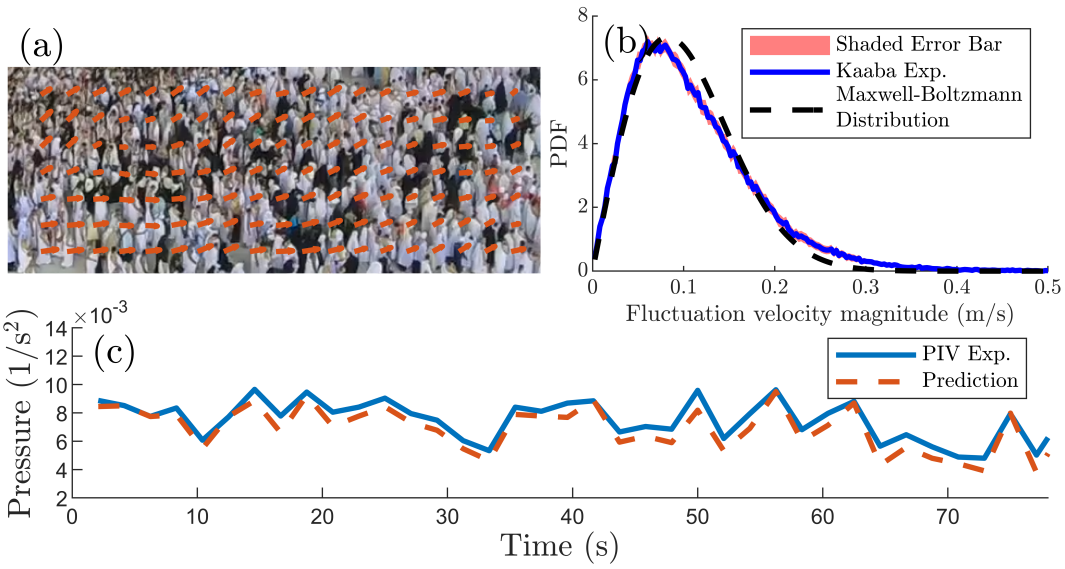

FIG. 3. (a) Single video frame illustrating a dense crowd with overlaid velocity vectors from PIV [19]. To facilitate comparisons, the image is not correct for perspective distortions. (b) The measured PDF for fluctuation velocity magnitude from the same video (blue line) and the best fit to a 2D Maxwell-Boltzmann distribution (black dashed line). The shaded area represents the error bar with 95% confidence interval. (c) Pressure change in the interrogation domain. Directly measured pressure from PIV is in the blue line. The pressure prediction from A, N, and k_BT is in the red dashed line.

emerge because the passive part of the system overcomes the self-propelling part of the system and expect that the equilibrium characteristic will emerge if $\tau \gg t_c$. However, this is not true. Equilibrium characteristics depend only on t_c and can emerge even the $\tau/t_c \approx 1$ as suggested by our experimental and modeling results. As our explanation in the previous paragraph suggests, as long as there is a sufficient amount of collision before significant temperature change, the active particle system will mimic an equilibrium system in the canonical ensemble fashion, and this is independent τ. Part of the reason is that we only consider fluctuation velocity. The self-driven part of the system contributes mainly to the mean velocity. This also explains why previous research only found equilibrium characteristics of jammed human crowds because jammed human crowds have a mean velocity around zero [18]. Our results reveal that, once the mean flow is removed, the equilibrium characteristics can exist in crowds even with strong self-propelling forces and mean flows.

The next natural question is whether there is a state variable that can be used as an indicator for the emergence of equilibrium characteristics in human crowds. Since $\rho \approx 1/r^2$ where r is the average distance between neighboring individuals, we can rewrite the collision time scale as $t_c = 1/(2\rho r\langle\|\mathbf{v}'\|\rangle) \propto r/\langle\|\mathbf{v}'\|\rangle$. Using the kinematic argument, we define the pressure of a crowd as $p = \rho\langle\mathbf{v}'^2\rangle/2$ [1, 2]. Similarly, we can rewrite pressure as $p = \rho\langle\mathbf{v}'^2\rangle/2 \propto \langle\mathbf{v}'^2\rangle/r^2$. It is obvious to see that $p \propto t_c^{-2}$. This is true under two conditions. First, individuals are relatively uniformly distributed ($\rho \approx 1/r^2$). Second, the variance of the fluctuation velocity magnitude is not too large ($\langle\mathbf{v}'^2\rangle \approx \langle\|\mathbf{v}'\|\rangle^2$), which means that k_BT should not be too large. This power law relationship is confirmed by both experimental and modeling results (Fig. 2a). Since there is a power law relationship between t_c and the mean squared error between fluctuation velocity magnitude PDFs and their best 2D Maxwell-Boltzmann fit, we know that the mean squared error will also have a power law relationship with pressure (Fig. 2b). Hence, high pressure indicates that the crowd system exhibits equilibrium characteristics.

The expression of $p = \rho\langle\mathbf{v}'^2\rangle/2$ indicates that the pressure of a crowd is a function of crowd density and the magnitude of fluctuation velocity. In other words, pressure is a function of crowd density and crowd temperature. The temperature of the crowd cannot vary too much because of the finite mobility of the individuals. Hence, the pressure of the crowd is mainly varied by the density of the crowd. Thus, high pressure is manifested by the high density of the human crowd. This is consistent with our observation that the equilibrium characteristics emerge in packed crowd systems.

B. Equipartition

In the context of equilibrium thermodynamics, for instance, the temperature of a system is intricately linked to the number of d.o.f. through the concept of equipartition, whereby each d.o.f. contributes an energy of $1/2k_BT$. For both experiments and modeling, we can write the kinetic energy as $E_k(t) = \mathbf{v}'^2/2$. We demonstrate that at high pressure, both experiments and mod-

eling with different boundary conditions and force potentials show that the equipartition holds very well for kinetic energy for different numbers of individuals N. The slope of the $2E_k/(k_BT)$ is well approximated as $2N$, indicating that each individual has two translational d.o.f. Our results indicate that human crowds under large pressure also follow the equipartition theorem.

Unlike the classical counterpart, i.e., the ideal gas, our system also stores potential energy. We can only calculate potential energy for the simulation system because the potential functions between individuals are unknown in experiments. While we can't calculate potential energy for experimental systems due to unknown potential functions between individuals, for simulations, we can write potential energy $E_p(t) = \lim_{T\to\infty} \frac{1}{T}\int_0^T dt[\frac{1}{2}\sum_{i\neq j} V_{ij}(\|\mathbf{r}_{ij}\|)]$. We find that the potential energy does not follow the equipartition theorem and is much larger than the kinetic energy. This observation is not unexpected. As the system has a high density and both exponential potential ($V_{ij}(\|\mathbf{r}_{ij}\|) = V_{ij}^0 e^{-\|\mathbf{r}_{ij}\|/R_{i,j}}$) and Lennard-Jones-like potential ($V_{ij}(\|\mathbf{r}_{ij}\|) = \epsilon((\frac{\sigma}{\|\mathbf{r}_{ij}\|})^{2n} - (\frac{\sigma}{\|\mathbf{r}_{ij}\|})^{n})$) reveals that the potential energy increase as distances between individuals decrease, the packed system will have very large potential energy associated with each individual.

We want to comment on the similarity and difference between high-pressure crowds and their classical counterparts. The similarity lies in the fact that the Maxwell-Boltzmann distribution, which describes the velocities of individual particles, arises from a canonical ensemble setup where each particle (or agent in the crowd) is treated as a system in thermal equilibrium with the rest of the particles that act as a reservoir. Energy transfer between the system and the reservoir occurs through interactions between particles, which may include collisions or other forms of interaction. Despite these individual energy changes, the overall energy distribution across all systems adheres to the Maxwell-Boltzmann statistics. This distribution is the most probable macrostate under the assumption of equal a priori probabilities for all accessible microstates, a fundamental principle in statistical mechanics.

A significant distinction between these systems lies in the motion of constituent particles between collisions. In a traditional gas system, molecules move with constant velocity along a given direction between collisions, assuming the absence of external forces, with their motion governed by their kinetic energy. These molecules perpetually move randomly, with their collisions emerging from this stochastic motion. Conversely, in a crowd system, the collisions between individuals are a consequence of the densely packed crowd and strong social forces [20, 26], which effectively results in a small collision time scale. This key difference in the motion of the particles between collisions makes the key difference in the condition for equipartition behavior. In a traditional gas system, equipartition assumes sparse molecules with negligible interactions. However, for a human crowd system to exhibit equipartition, the individuals are densely packed and continuously interacting.

IV. THE IDEAL GAS LAW AND IT'S APPLICATION

A. The Ideal Gas Law as the Equation of State for Crowd with High Pressure

Given the fact that the individual's fluctuation velocity magnitude follows the 2D Maxwell-Boltzmann distribution, we can analytically integrate the 2D Maxwell-Boltzmann distribution to evaluate $\langle \mathbf{v}'^2 \rangle$, and plug it into the expression of pressure ($p = \rho\langle \mathbf{v}'^2 \rangle/2$). Thus, we derived the two-dimensional equivalent of the ideal gas law for human crowds subjected to high pressure

$$pA = Nk_BT \tag{6}$$

where A is the area of interest, N is the number of particles, k_B is Boltzmann constant and T is the temperature. This result is highly nontrivial because it reveals that, under high pressure, human crowds, as an inherently non-equilibrium system, are governed by an equation of state mimicking the ideal gas law.

The ideal gas law for human crowds illuminates intriguing parallels between high-pressure crowd behaviors and principles of equilibrium thermodynamics. This perspective opens avenues to explore and validate traditional thermodynamic quantities and laws within the context of high-pressure human crowds, advancing our understanding of this active matter system. For instance, straightforward derivations yield the heat capacity of a high-pressure crowd at constant area as $C_A = k_BN$, and at constant pressure as $C_P = 2k_BN$.

The ideal gas law relates four state variables (p, A, N, and T) and has several important applications, and we just name a few here. Similar to calculating the number of gas molecules in stoichiometry, the ideal gas law for a human crowd can be used to accurately estimate the number of individuals in an extremely dense crowd, which is a highly valuable yet challenging task [31, 32]. With the velocity fluctuation information from standard particle image velocimetry (PIV) analysis [33, 34], one can easily calculate the number of individuals via ideal gas law. Second, using an ideal gas law for crowds could provide a mathematical basis to predict potentially dangerous situations, like stampedes or panics. Previous research has shown that the stampedes are usually preceded by high pressure in the crowd [2]. For instance, the ideal gas law reveals that the pressure of the crowd is inversely proportional to the area given that the temperature and the number of individuals are fixed. This simply implies that special care should be taken in the area where contraction happens. In the following section, we will show the application of the ideal gas law for the human crowd with high pressures.

B. Application of the Ideal Gas Law

The ideal gas law offers a powerful way to predict the state variables. Its efficacy is highlighted through a variety of video data available on YouTube.com, which demonstrates its applicability in numerous contexts. Our findings reveal that the ideal gas law accurately predicts pressure levels in all instances of high-pressure crowds, underpinning its versatile applicability. In addition, we drive a crowd in a thermodynamic cycle in the agent-based model and predict the system pressure with the ideal gas law, showing the predicting power of the ideal gas law.

To demonstrate our ideal gas law, we examined additional sets of dense human crowd videos on YouTube.com (Fig. 3), all filmed from an elevated perspective to offer a top-down view. We find that our model accurately predicts the pressure for all dense (high-pressure) crowds.

We correct the perspective distortion [35] and use PIV analysis [33, 34] to measure the 2D velocity fields on an interpolated grid. Here, we show the PIV result and pressure prediction using the ideal gas law for one of the data sets. Fig. 3a shows the raw image data with the overlaid velocity field. This image is not corrected for perspective distortion to facilitate the visual comparison. We show that the fluctuation velocity magnitude of the packed system also approximates Maxwell-Boltzmann distribution (Fig. 3b). Using Eqn. 6, we predict the pressure value based on A, N, and k_BT where k_BT is gotten from fitting the fluctuation velocity magnitude's PDF. We see that pressure prediction is accurate. For a variety of high-pressure crowd video data, our ideal gas law consistently performs well.

The power of the ideal gas law as an equation of state lies in its ability to describe how state variables change when some are varied while the system remains in a constant state, such as in the case of an engine [36]. To demonstrate that our ideal gas law can similarly describe human crowds, it is necessary to drive them away from their natural state. We achieve this by simulating a crowd passing through a long corridor with a variable width, as depicted in Fig. 4 a. We simulated a corridor of 400 m in length. The width between 100 m and 300 m is 10 m. The first 100 m and the last 100 m are contraction and expansion, respectively. The side walls are half of a Gaussian function $h(x) = A/(\sqrt{2\pi}\alpha)\mathrm{e}^{-\frac{(x-\mu)^2}{2\alpha^2}}$ with $A = 200$, $\alpha = 45$ m, and μ is 0 or 400 m. The widest width is 13.55 m. We simulated 3,000 individuals passing to the right with a periodic boundary condition. We choose Lennard-Jones-like potential (Eqn. 4) with $\epsilon = 3$, $n = 0.5$, and $\sigma = 2.4$ m. The analysis focuses on a convex hull moving from left to right with the mean flow of the crowd. We initiate a random convex hull enclosing 150 individuals within a 50 m $\times$ 5 m region on the left side. In the next time step, we find the center of the convex hull based on the new positions of the 150 individuals. Then, we find the nearest 150 individuals around the center and form a new convex hull. The simulation ends when the convex hull arrives at the right side of the corridor.

Given that we do not observe any evidence of a phase transition, we would expect the ideal gas law to remain valid throughout the entire cycle. To test this, we used simulated A, N, and k_BT to predict the pressure p. As shown in Fig. 4 b and c, the predicted pressure closely matches the simulated data. These results provide compelling evidence that the ideal gas law is a valid equation of state for human crowds with high pressure.

V. SUMMARY AND DISCUSSION

The present study investigated human crowds as a form of active matter, where individuals convert internal energy into motion. Notably, such crowds can display equilibrium characteristics, analogous to those observed in the field of thermodynamics. The research aimed to understand the conditions and reasons that enable human crowds to exhibit equilibrium characteristics and to investigate if an equation of state could be formulated for crowd dynamics.

This study discovered that human crowds tend to exhibit equilibrium characteristics as the collision timescale between individuals decreases. This was consistently observed across various social forces and motion cases. Remarkably, it persisted even in the presence of strong self-propulsion. A power law relationship between collision timescale and pressure was also found, suggesting that higher pressure indicated to equilibrium behavior. Furthermore, it was shown that under high pressure, human crowds followed the equipartition theorem, leading to the formulation of an ideal gas law for crowds. We demonstrated the applicability of the ideal gas law to human crowds through a variety of crowd video data and modeling of a crowd in a thermodynamic cycle.

The findings present a novel perspective on understanding human crowds as a form of active matter, showing potential parallels between the behaviors of high pressure crowds and equilibrium thermodynamics. The ideal gas law application to crowds could be a substantial step towards a more profound comprehension of crowd dynamics under high pressure. First, this paper only defines the pressure kinematically. The future work includes adding leading order virial terms to define pressure dynamically. One has to meticulously measure the realistic potential function between individuals and determine whether the leading order virial term is negligible. In the case where the virial term is not negligible, it will lead to a crowd of individuals interacting with a Lennard-Jones potential to have a van der Waals-like equation of state. Second, one could further define thermodynamic variables for human crowds with high pressure. Third, one could explore the analogous laws in thermodynamics for the human crowd under high pressure, such as the first and second laws of thermodynamics. Last, one can study

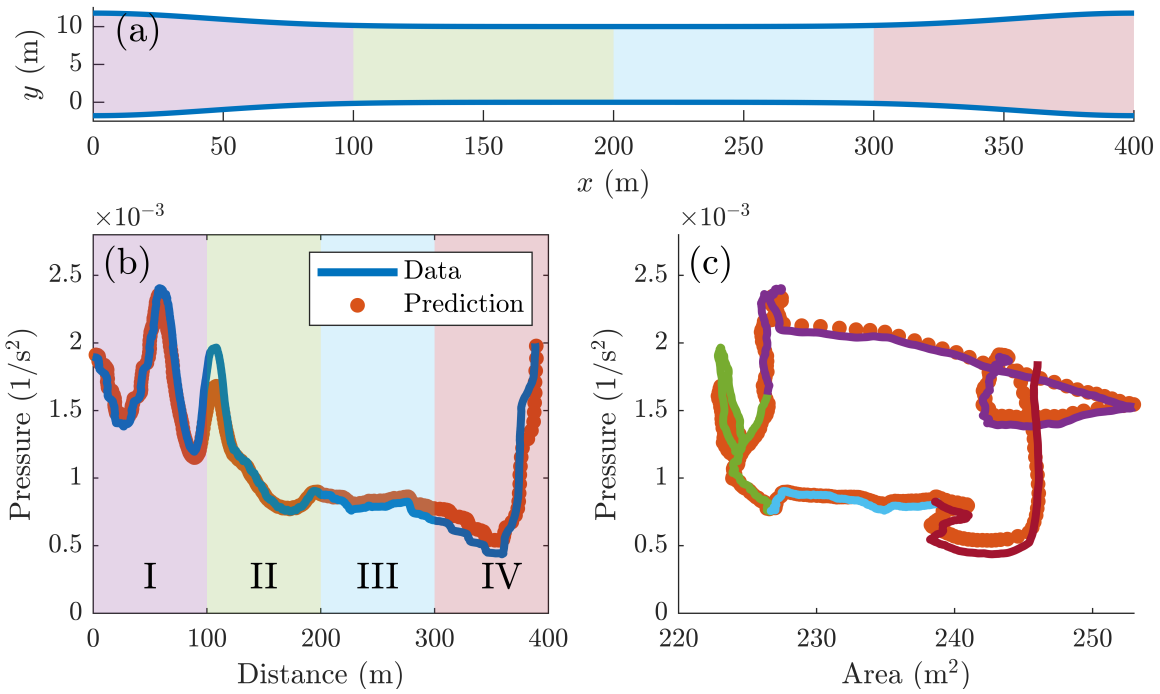

FIG. 4. Thermodynamic cycling of the human crowd. (a) A snapshot of the corridor with variable width. (b) The phase averaged pressure change inside a convex hull along the corridor (blue line) and the pressure prediction via the ideal gas law (red dots). (c) Phase-averaged pressure-area phase plane behavior while the crowd passes the corridor. The solid lines represent the hydrodynamic cycle with simulated data, and the red dots are the cycle with the predicted pressure. Totally 10 cycles were used for phase averaging. Data has also been averaged every 1 s for clarity.

how to apply these laws and defined variables to facilitate better the efficiency and comfort of the transport of human crowds.

[1] M. Moussaïd, D. Helbing, and G. Theraulaz, How simple rules determine pedestrian behavior and crowd disasters, Proceedings of the National Academy of Sciences **108**, 6884 (2011).

[2] D. Helbing, A. Johansson, and H. Z. Al-Abideen, Dynamics of crowd disasters: An empirical study, Physical review E **75**, 046109 (2007).

[3] D. Helbing and P. Molnar, Social force model for pedestrian dynamics, Physical review E **51**, 4282 (1995).

[4] I. D. Couzin and N. R. Franks, Self-organized lane formation and optimized traffic flow in army ants, Proceedings of the Royal Society of London. Series B: Biological Sciences **270**, 139 (2003).

[5] G. C. Dachner and W. H. Warren, Behavioral dynamics of heading alignment in pedestrian following, Transportation Research Procedia **2**, 69 (2014).

[6] N. T. Ouellette, Flowing crowds, Science **363**, 27 (2019).

[7] T. Vicsek and A. Zafeiris, Collective motion, Physics reports **517**, 71 (2012).

[8] M. Isobe, D. Helbing, and T. Nagatani, Experiment, theory, and simulation of the evacuation of a room without visibility, Physical Review E **69**, 066132 (2004).

[9] D. Helbing, M. Isobe, T. Nagatani, and K. Takimoto, Lattice gas simulation of experimentally studied evacuation dynamics, Physical review E **67**, 067101 (2003).

[10] D. Helbing, I. Farkas, and T. Vicsek, Simulating dynamical features of escape panic, Nature **407**, 487 (2000).

[11] D. Helbing, I. J. Farkas, and T. Vicsek, Freezing by heating in a driven mesoscopic system, Physical review letters **84**, 1240 (2000).

[12] F. Peruani, T. Klauss, A. Deutsch, and A. Voss-Boehme, Traffic jams, gliders, and bands in the quest for collective motion of self-propelled particles, Physical Review Letters **106**, 128101 (2011).

[13] I. Karamouzas, B. Skinner, and S. J. Guy, Universal power law governing pedestrian interactions, Physical review letters **113**, 238701 (2014).

[14] A. Bottinelli, D. T. Sumpter, and J. L. Silverberg, Emergent structural mechanisms for high-density collective motion inspired by human crowds, Physical review letters **117**, 228301 (2016).

[15] N. Bain and D. Bartolo, Dynamic response and hydrodynamics of polarized crowds, Science **363**, 46 (2019).

[16] H. L. Devereux and M. S. Turner, Environmental path-

entropy and collective motion, Physical Review Letters **130**, 168201 (2023).
[17] L. Henderson, The statistics of crowd fluids, nature **229**, 381 (1971).
[18] J. L. Silverberg, M. Bierbaum, J. P. Sethna, and I. Cohen, Collective motion of humans in mosh and circle pits at heavy metal concerts, Physical review letters **110**, 228701 (2013).
[19] Over one million videos are available on youtube.com illustrating crowd with high pressure. notable examples include https://www.youtube.com/watch?v=l-yyr1on66w (2023).
[20] X. Si and L. Fang, A novel social distance model reveals the sidewall effect at bottlenecks, Scientific reports **11**, 20982 (2021).
[21] C. Feliciani, I. Zuriguel, A. Garcimartín, D. Maza, and K. Nishinari, Systematic experimental investigation of the obstacle effect during non-competitive and extremely competitive evacuations, Scientific reports **10**, 1 (2020).
[22] S. Cao, A. Seyfried, J. Zhang, S. Holl, and W. Song, Fundamental diagrams for multidirectional pedestrian flows, Journal of Statistical Mechanics: Theory and Experiment **2017**, 033404 (2017).
[23] N. Mordant, A. M. Crawford, and E. Bodenschatz, Experimental lagrangian acceleration probability density function measurement, Physica D: Nonlinear Phenomena **193**, 245 (2004).
[24] N. Mordant, A. M. Crawford, and E. Bodenschatz, Three-dimensional structure of the lagrangian acceleration in turbulent flows, Physical Review Letters **93**, 214501 (2004).
[25] F. Toschi and E. Bodenschatz, Lagrangian properties of particles in turbulence, Annual Review of Fluid Mechanics **41**, 375 (2009).
[26] D. Helbing and P. Molnar, Social force model for pedestrian dynamics, Physical review E **51**, 4282 (1995).
[27] X. Chen, M. Treiber, V. Kanagaraj, and H. Li, Social force models for pedestrian traffic–state of the art, Transport reviews **38**, 625 (2018).
[28] A. Cavagna, A. Cimarelli, I. Giardina, G. Parisi, R. Santagati, F. Stefanini, and M. Viale, Scale-free correlations in starling flocks, Proceedings of the National Academy of Sciences **107**, 11865 (2010).
[29] X. Chen, X. Dong, A. Be'er, H. L. Swinney, and H. Zhang, Scale-invariant correlations in dynamic bacterial clusters, Physical review letters **108**, 148101 (2012).
[30] S. J. Blundell and K. M. Blundell, *Concepts in thermal physics* (Oxford University Press on Demand, 2010).
[31] B. Zhan, D. N. Monekosso, P. Remagnino, S. A. Velastin, and L.-Q. Xu, Crowd analysis: a survey, Machine Vision and Applications **19**, 345 (2008).
[32] H. Idrees, I. Saleemi, C. Seibert, and M. Shah, Multi-source multi-scale counting in extremely dense crowd images, in *Proceedings of the IEEE conference on computer vision and pattern recognition* (2013) pp. 2547–2554.
[33] W. Thielicke and R. Sonntag, Particle image velocimetry for matlab: Accuracy and enhanced algorithms in pivlab, j. open res. softw., 9 (2021).
[34] W. Thielicke and E. J. Stamhuis, Pivlab-time-resolved digital particle image velocimetry tool for matlab, Published under the BSD license, programmed with MATLAB **7**, R14 (2014).
[35] C. Py, E. de Langre, B. Moulia, and P. Hémon, Measurement of wind-induced motion of crop canopies from digital video images, Agricultural and forest meteorology **130**, 223 (2005).
[36] M. Sinhuber, K. van der Vaart, Y. Feng, A. M. Reynolds, and N. T. Ouellette, An equation of state for insect swarms, Scientific Reports **11**, 3773 (2021).